The structural basis of differential inhibition of human calpain by indole and phenyl a-mercaptoacrylic acids

Sarah E. Adams [a], Pierre J. Rizkallah [b], David J. Miller [a], Emma J. Robinson [b], Maurice B. Hallett [b], Rudolf K. Allemann [a,⇑]

[a] School of Chemistry, Main Building, Cardiff University, Park Place, Cardiff CF10 3AT, UK
[b] School of Medicine, Institute of Molecular and Experimental Medicine, Heath Park, Cardiff University, Cardiff CF14 4XN, UK

article info

Keywords:
Calpain-I
Mercaptoacrylic acids
PEF(S)
Rheumatoid arthritis

abstract

Excessive activity of neutrophils has been linked to many pathological conditions, including rheumatoid arthritis, cancer and Alzheimer's disease. Calpain-I is a Ca^{2+}-dependent protease that plays a key role in the extravasation of neutrophils from the blood stream prior to causing damage within affected tissues. Inhibition of calpain-I with small molecule mercaptoacrylic acid derivatives slows the cell spreading pro-cess of live neutrophils and so these compounds represent promising drug leads. Here we present the 2.05 and 2.03 Å co-crystal X-ray structures of the pentaEF hand region, PEF(S), from human calpain with (Z)-3-(4-chlorophenyl)-2-mercaptoacrylic acid and (Z)-3-(5-bromoindol-3-yl)-2-mercaptoacrylic acid. In both structures, the a-mercaptoacrylic acid derivatives bind between two a-helices in a hydrophobic pocket that is also exploited by a leucine residue of the endogenous regulatory calpain inhibitor calpast-atin. Hydrophobic interactions between the aromatic rings of both inhibitors and the aliphatic residues of the pocket are integral for tight binding. In the case of (Z)-3-(5-bromoindol-3-yl)-2-mercaptoacrylic acid, hydrogen bonds form between the mercaptoacrylic acid substituent lying outside the pocket and the pro-tein and the carboxylate group is coplanar with the aromatic ring system. Multiple conformations of (Z)-3-(5-bromoindol-3-yl)-2-mercaptoacrylic acid were found within the pocket. The increased potency of (Z)-3-(5-bromoindol-3-yl)-2-mercaptoacrylic acid relative to (Z)-3-(4-chlorophenyl)-2-mercaptoacrylic acid may be a consequence of the indole group binding more deeply in the hydrophobic pocket of PEF(S) than the phenyl ring.

1. Introduction

The calpain family includes 15 known calcium activated cys-teine proteases (Sorimachi et al., 2011), of which calpain-I and cal-pain-II are the two best-studied isoforms (Campbell and Davies, 2012; Sorimachi et al., 2011). They are heterodimeric proteins expressed in the cytosol and comprised of a large (80,000 M_r) and a small subunit (30,000 M_r). The large subunit contains the active site within the CysPc domain along with a calcium binding domain, PEF(L), a postulated phospholipid binding domain (C2L) and a N-terminal anchor helix (Sorimachi et al., 2011). The small subunits (CAPNS1) of calpain-I and calpain-II are identical (Ohno et al., 1986). CAPNS1 is composed of a glycine rich domain and a second calcium binding domain, PEF(S). The large subunit varies significantly between the two isoforms with an overall sequence identity of 62% (Imajoh et al., 1988). The concentration of calcium that is required for activation in vitro is 50 lM and 0.35 mM for cal-pain-I and calpain-II, respectively (Goll et al., 2003).

Numerous functions have been postulated for calpain-I and cal-pain-II in the human body with links to signal transduction (Sato and Kawashima, 2001), cell motility (Hallett and Dewitt, 2007), apoptosis (Harwood et al., 2005; Orrenius et al., 2003) and the cell cycle (Schollmeyer, 1988; Zhang et al., 1997). The lack of availabil-ity of isoform specific calpain inhibitors has hindered elucidation of their exact physiological roles. Calpain-I and calpain-II are both inhibited by the regulatory endogenous protein calpastatin (Wendt et al., 2004). Calpastatin contains four inhibitory domains and each of these domains is capable of inactivating one molecule of calpain (Emori et al., 1987; Hanna et al., 2007). Each inhibitory domain is composed of three binding regions that bind to different regions of the heterodimeric protease (Hanna et al., 2008). Regions A and

Abbreviations: CAPNS1, calpain small subunit; DTT, dithiothreitol; PEF(S) and PEF(L), pentaEF hand subunits (domain VI and IV) of calpains I and II.

⇑ Corresponding author. Fax: +44 (0) 29 208 74030. E-mail address: allemannrk@cardiff.ac.uk (R.K. Allemann).

C bind to the calcium binding domains PEF(L) and PEF(S), respec-tively, and region B binds to the CysPc domain (Hanna et al., 2008; Maki et al., 1987).

Decreased levels of calpastatin as well as over-activation of cal-pain-I are linked to a wide variety of pathological conditions. These include Alzheimer's disease (Saito et al., 1993), rheumatoid arthritis (Miller et al., 2013), cancer (Storr et al., 2011) and ischemic cell death (Tontchev and Yamashima, 1999). Calpain I mediates the cell spreading behaviour of neutrophils, a necessary prelude to their extravasation through the blood vessel wall and migration towards pathogens or sites of tissue damage (Hallett and Dewitt, 2007). Hence calpain-I is a potential target for small molecule intervention (Miller et al., 2013). Previously, we have reported the synthesis of a series of cell permeable a-mercaptoacrylic acid derivatives that act as potent inhibitors of calpain-I and cause decreased rates of cell spreading in live neutrophils (Adams et al., 2012). We now report the binding mode of two a-mercaptoacrylic acid derivatives with the calcium binding domain of human PEF(S). PEF(S) is composed of nine a-helices that fold to form five EF-hands. Four of these EF-hands bind calcium and the fifth is used to form the heterodimeric interface with the corrresponding EF-hand of PEF(L) of the large sub-unit (Hosfield et al., 1999; Strobl et al., 2000). Alone PEF(S) forms a dimer with two EFH5 binding to its respective partner (Blanchard et al., 1997; Lin et al., 1997b; Todd et al., 2003). We have previously shown that halogenated indole mercaptoacrylates are more potent allosteric calpain inhibitors than their phenyl analogues (Adams et al., 2012). To understand the molecular basis of this observation, we now compare the co-crystal structures of PEF(S) with (Z)-3-(4-chlorophenyl)-2-mercaptoacrylic acid and (Z)-3-(5-bromoindol-3-yl)-2-mercaptoacrylic acid. The indole group binds more deeply in the hydrophobic pocket of PEF(S) of human calpain, which suggests a mechanism for the generally increased potency of all indole-based inhibitors over their phenyl counterparts.

2. Materials and methods

(Z)-3-(4-Chlorophenyl)-2-mercaptoacrylic acid (1) and (Z)-3-(5-bromoindol-3-yl)-2-mercaptoacrylic acid (2) were prepared as described previously (Adams et al., 2012).

2.1. Expression, purification and crystallisation of PEF(S)

The codon optimised gene encoding human PEF(S) was pur-chased from Epoch Biolabs (Texas, USA) in a pET21d vector. Human PEF(S) was produced in Escherichia coli BL21-CodonPlus(DE3)-RP (Agilent Technologies) and purified and crystallized using the same procedure previously described the for PEF(S) from Sus scrofa (Lin et al., 1997a). The crystals took approximately one week to grow. Prior to data collection ethylene glycol was added to the drop con-taining the crystals to a total concentration of 20% (w/v). The crys-tals were then harvested and flash frozen in liquid nitrogen.

Soaking the inhibitors into the preformed crystals of PEF(S) was carried out 24 h prior to the harvesting of crystals. 16 mM Solu-tions of (Z)-3-(5-bromoindol-3-yl)-2-mercaptoacrylic acid and (Z)-3-(4-chlorophenyl)-2-mercaptoacrylic acid in the precipitant solution (50 mM sodium cacodylate, 12.5% PEG6000, 20 mM cal-cium chloride and 10 mM DTT at pH 7.0) were prepared immedi-ately before soaking. 1 ll of the 16 mM solutions were added to the drops containing the crystals to a total concentration of 2 mM in the drop.

2.2. Data collection and phasing

The diffraction data were collected at Diamond Light Source (Oxford, UK, beamlines I03 and I04-1) at a temperature of 100 K. The wavelengths used for diffraction were 0.920 Å (unliganded-PEF(S)) and 0.976 Å (PEF(S)-1, PEF(S)-2) with a Pilatus pixelated detector. The raw diffraction images were processed through the xia2 data-reduction system (Winter, 2010). The data were scaled, reduced and analysed using Scala (Evans, 2006) and Aimless (Evans and Murshudov, 2013) from the CCP4i package (Collabora-tive Computational Project number 4) (Potterton et al., 2003).

2.3. Molecular replacement and refinement

The structures were solved with molecular replacement using Phaser (CCP4i) (McCoy, 2007). The search model was derived from the structure of PEF(S) (PDB:1ALV) (Lin et al., 1997b; McCoy, 2007). The solution obtained was adjusted with the COOT program (Crys-tallographic Object-Oriented Toolkit) (Emsley and Cowtan, 2004) for molecular model building and completion, and the model was refined further with the Refmac5 refinement program (Murshudov et al., 1997). The models for the small molecules 1 and 2, were created with ProDrg (Schuttelkopf and van Aalten, 2004).

3. Results and discussion

The data collection and refinement statistics for human PEF(S) and PEF(S) complexed with 1 and 2 are reported in Table 1. The structure of porcine unliganded-PEF(S) was also determined for completeness (Table S1). The resolutions were 1.60 Å for PEF(S) and 2.03–2.05 Å for the two co-crystal structures.

Table 1
The data statistics for the structures of unliganded-PEF(S), PEF(S)-1 and PEF(S)-2.

Crystal form	Unliganded-PEF(S)	PEF(S)-1	PEF(S)-2
Data collection			
X-ray source	DLS I04-1	DLS I03	DLS I03
Wavelength (Å)	0.9200	0.9673	0.9673
Space group	$P12_11$	$P12_11$	$P12_11$
Unit cell a (Å)	49.63	49.54	49.41
b (Å)	79.31	80.09	79.34
c (Å)	57.10	56.89	57.26
Wilson B-factor (A^2)	20.0	26.6	30.1
Resolution (Å)	49.61–1.60 (1.64–1.60)	80.09–2.05 (2.10–2.05)	41.93–2.03 (2.08–2.03)
Unique reflections	51,828 (3589)	25,589 (3670)	27,196 (1648)
Multiplicity	4.1 (4.2)	3.4 (2.6)	3.5 (2.7)
Completeness (%)	89.0 (83.8)	91.8 (70.0)	95.0 (78.4)
Mean I/rI	12.7 (2.3)	10.8 (2.3)	17.9 (2.4)
$CC_{1/2}$	0.997 (0.769)	0.977 (0.650)	0.994 (0.497)
R_{merge} (%)	5.9 (60.6)	8.3 (103.9)	5.1 (111.5)
Refinement			
Resolution (Å)	49.61–1.60	80.09–2.05	41.93–2.03
No. reflections	49,154	24,048	25,811
R_{work} (%)	16.6	23.1	19.7
R_{free} (%)	20.1	27.9	25.1
No. of non H atoms			
Protein	2952	2816	2806
Ligand/ion	8	34	56
Water	387	141	150
Average B-factor (A^2)			
Protein	24.7	39.5	44.4
Ions	22.0	35.4	40.6
Ligand		78.2	79.5
Water	34.8	41.4	46.6
r.m.s.deviations			
Bond length (Å)	0.019	0.016	0.019
Bond angles (L)	1.858	1.742	2.007
Ramachandran plot			
Favoured (%)	98.9	99.1	98.5
Allowed (%)	100	100	100
Number of Outliers	0	0	0
PDB code	4PJH	4PHK	4PHM

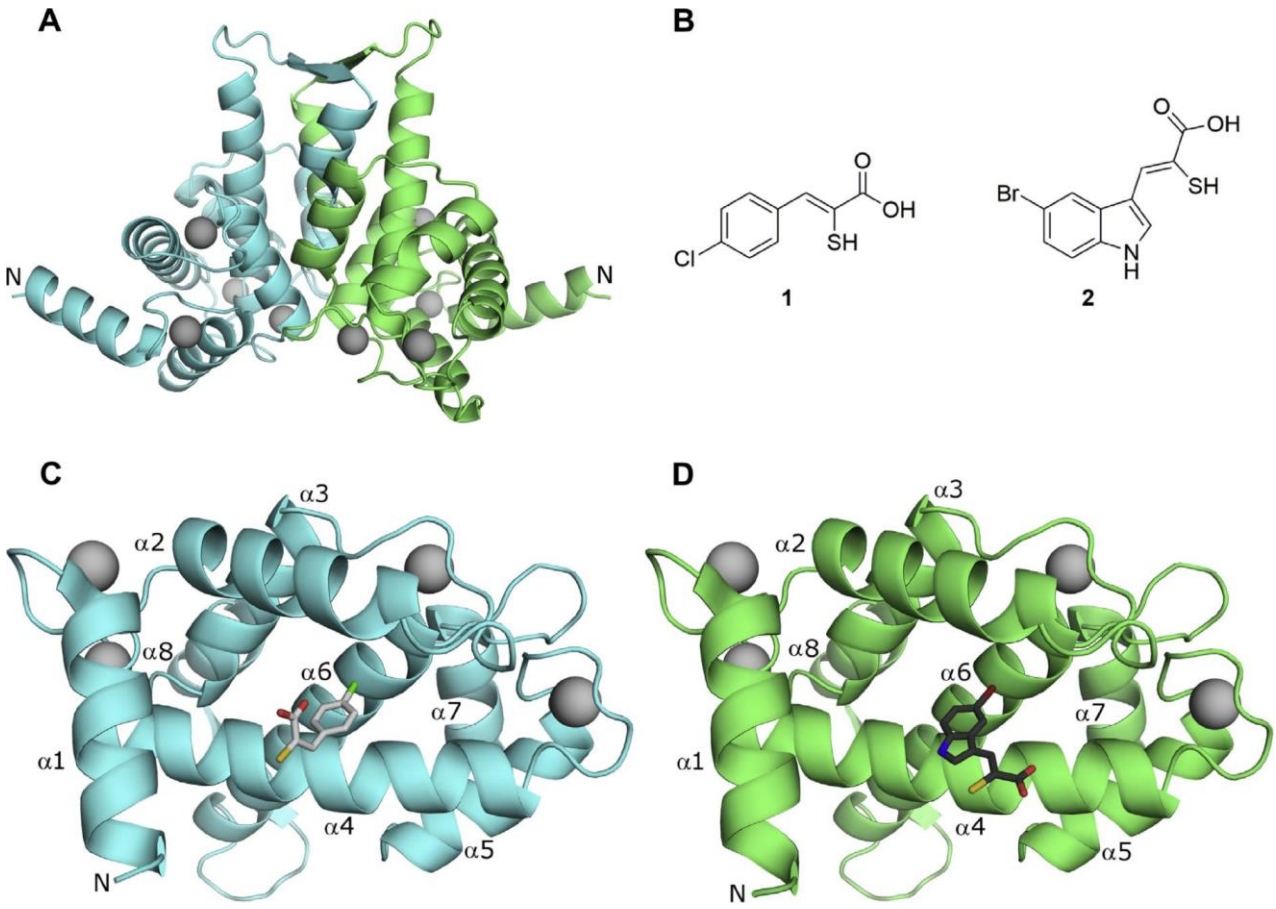

Fig.1. (A) Cartoon representation of the calcium bound homodimer of human PEF(S); chain A is cyan and chain B is green, calcium ions are represented as grey spheres, the N-terminus of each monomer is labelled. (B) The structures of 1 ((Z)-3-(5-bromoindol-3-yl)-2-mercaptoacrylic acid) and 2 ((Z)-3-(4-chlorophenyl)-2-mercaptoacrylic acid).
(C) Compound 1 (stick model) bound to chain A of PEF(S), with the a-helices labelled from the N-terminus. (D) Compound 2 (stick model) bound to chain B of PEF(S), (PDB: 4PHJ, 4PHK and 4PHM), with the a-helices labelled from the N-terminus.

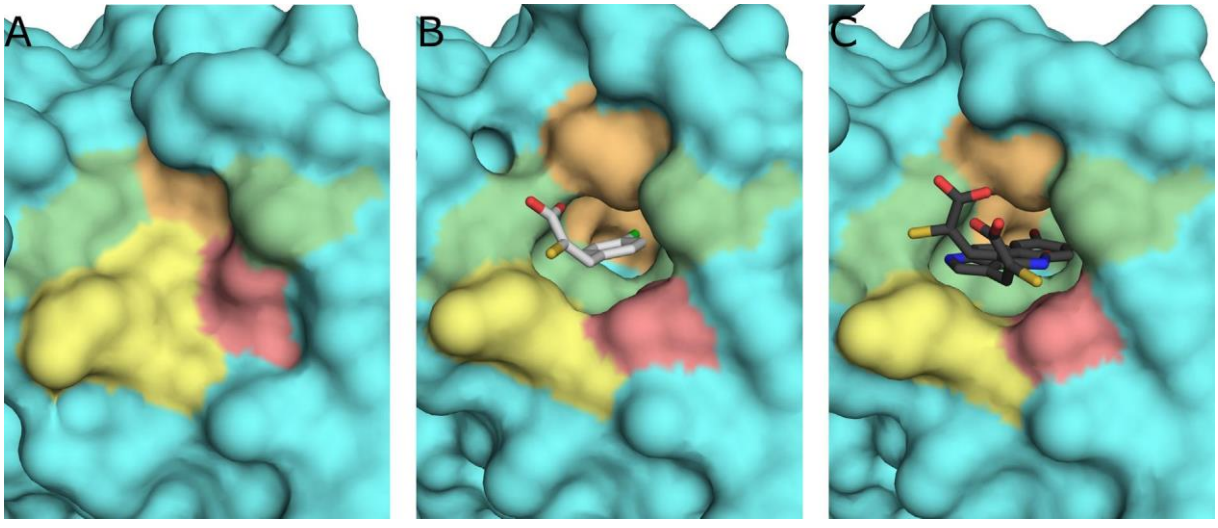

Fig.2. A comparison of the surface at the a-mercaptoacrylic acid binding site of unliganded-PEF(S) (A), PEF(S)-1 (B) and PEF(S)-2 (C). Q175 in red (r.m.s.d. > 2), L124, V127 and V128 in orange (r.m.s.d > 1), H131, W168, I173 and F226 in green (r.m.s.d < 1). F139 is highlighted in orange and green in images B and C. There were two conformations of K172 (yellow) observed in A, one of which partially occupies the binding pocket (r.m.s.d value cannot be calculated).

3.1. Unliganded structure of PEF(S)

Previous structures of isolated PEF(S) have been derived from Sus scrofa (wild boar), while the structures discussed in this work are for human PEF(S). There is a difference of five amino acids between the human and porcine forms of PEF(S), namely K173R, V183T, G190C, S211N and G221S. These amino acids have little effect on the overall structure of PEF(S) as the refined structure

Table 2
The r.m.s.d. values for the side chains in the hydrophobic pocket of PEF(S) on binding of 1 and 2 to both chains in the homodimer (N/A = more than one conformation of the side chain in the unliganded-PEF(S)). Comparison between unliganded-PEF(S), PEF(S)-1 and PEF(S)-2 carried out using Superpose in the CCP4 package (Bailey, 1994).

Residue	Unliganded-PEF(S)/PEF(S)-1 r.m.s.d.		Unliganded-PEF(S)/PEF(S)-2 r.m.s.d.	
	Chain A (Å)	Chain B (Å)	Chain A (Å)	Chain B (Å)
L124	1.82	1.81	1.82	1.82
V127	1.28	1.50	1.42	1.40
V128	1.06	N/A	0.76	N/A
H131	0.32	0.53	0.31	0.24
F139	1.82	1.78	0.13	0.12
W168	0.64	0.43	0.63	0.22
I171	0.34	0.32	0.28	0.24
Q175	2.32	2.61	2.59	2.45
F226	0.27	0.26	0.18	0.18

of human PEF(S) showed a homodimer in the asymmetric unit that was closely related that of porcine PEF(S) (Lin et al., 1997b; Todd et al., 2003). EF hand 5 (EFH5) bound to its respective partner in the second monomer with a hydrophobic patch containing I254, V256, I258 and L262 interacting with their counterparts at the dimer interface. The other four EF-hands all bind calcium ions in agreement with the structure of the porcine homologue (Fig. 1) (Lin et al., 1997b; Todd et al., 2003).

3.2. PEF(S) with inhibitors bound

The two inhibitors (Z)-3-(4-chlorophenyl)-2-mercaptoacrylic acid (1) and (Z)-3-(5-bromoindol-3-yl)-2-mercaptoacrylic acid (2) both bind between the second and fourth a-helix of PEF(S) (Fig. 1). This pocket is also known to accommodate a leucine resi-due from the calpastatin binding region C and another a-merca-ptoacrylic acid PD150606 (Hanna et al., 2008; Lin et al., 1997b; Todd et al., 2003). To accommodate both ligands the side chain of Q175 that normally occupies this pocket is driven away to form a cavity for the ligand (Fig. 2). R.m.s.d. calculations of the side chains within the hydrophobic pocket using Superpose (Bailey, 1994) indicated that Q175 of protein chain A showed the most sig-nificant movement within the protein upon binding an inhibitor; the values for r.m.s.d. were 2.32 and 2.62 Å for 1 and 2, respectively (Table 2.). These values also indicate that L124 and V127 signifi-cantly alter their conformation upon ligand binding (Table 2.). L124 rotates and V127 shifts to accommodate the ligand. The refined structures indicate that the phenyl ring of F139 undergoes a translational shift on compound 1 binding but this shift is not observed in the complex of PEF(S) with 2 (Table 2).

The movement of these residues can be seen more clearly with a surface diagram of the protein (Fig. 2) as there is no hydrophobic pocket observed in the surface representation of unliganded-PEF(S), due to the pocket being filled by Q175, L124 and V127 (Fig. 2). In the presence of the inhibitors the residues within the

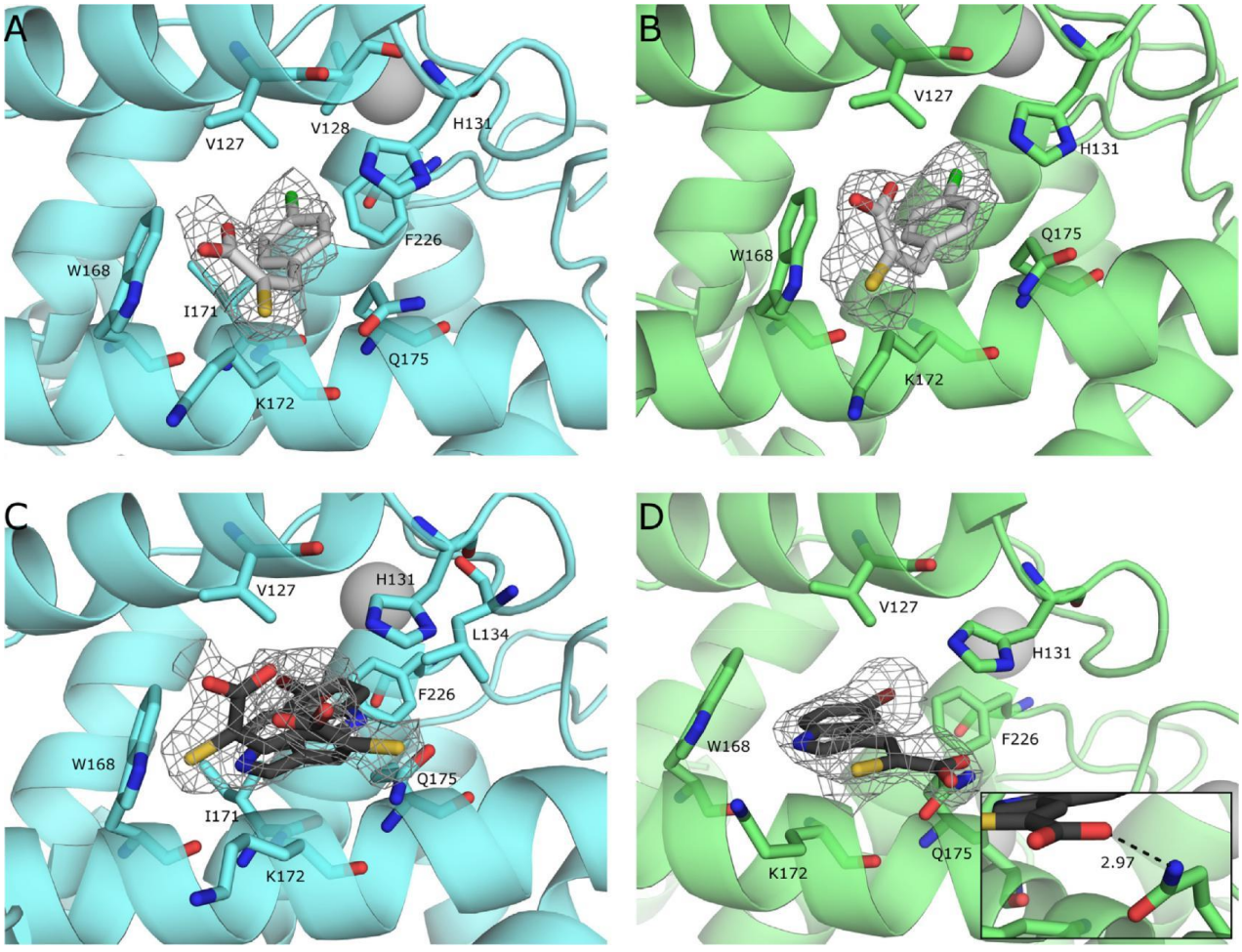

Fig.3. A comparison of the inhibitor 1 (light grey) in stick form bound to chain A (A) and chain B (B) and the inhibitor 2 (dark grey) in stick form bound to chain A (C) and chain B (D) of the homodimer represented in cartoon format with the residues within 4 Å of the inhibitor highlighted in stick form. Inset: notable hydrogen bond between Ne2 of Q175 and the carboxylate group of compound 2 (distance shown in Å). The density maps are contoured to 1r. (PDB: 4PHK and 4PHM).

pocket move to accommodate the aromatic rings of both 1 and 2 (Fig. 2). The volume of the pocket is dependent on the size of the aromatic ring and the pocket is slightly larger when 2 is bound (Fig. 2). In chain A of PEF(S)-2 two separate conformations of the ligand are visible within the pocket suggesting that the pocket might be able to accommodate ligands larger than indoles (Fig. 2).

The 4-chlorophenyl ring of 1 sits inside the hydrophobic pocket with the hydrophilic a-mercaptoacrylic acid substituent adopting a conformation perpendicular to the aromatic ring in chains A and B of the homodimer (Fig. 3). The majority of interactions are within the hydrophobic pocket itself. The CCP4i program Contact (Bailey, 1994) indicated that van der Waals (vdW) contacts are pre-dicted within 4 Å between the 4-chlorophenyl group and the alkyl chains of K173 and Q175 as well as H131, W168, L127, I171 and F226. No hydrogen bonds or other polar contacts were observed between the mercaptoacrylic acid substituent and the protein.

Compound 2 adopts two separate conformations in each of the monomers of PEF(S) in the asymmetric unit. In chain A, the elec-tron density map indicated that the a-mercaptoacrylic acid lies perpendicular to the aromatic ring in a conformation similar to that found for 1. In chain B on the other hand 2 the hydrophilic group is coplanar with the aromatic ring (Fig. 3). For chain A, 2 adopts two conformations in the hydrophobic pocket, with the indole ring flipped 180L relative to the other. Hence the NH group of the indole ring and the thiol of the mercaptoacrylic acid substi-tuent interact with different residues inside the pocket. There are over 50 vdW interactions between the residues within the hydro-phobic pocket and the two conformations of 2 in chain A. Fewer interactions were observed when the inhibitor lies in the fully pla-nar conformation within the pocket seen in chain B, despite the hydrogen bond that forms between the carboxylic acid and Ne2 of Q175, at 3.0 Å.

The size of the aromatic ring system is an important factor for determining the affinity of PEF(S) for the mercaptoacrylic acid inhibitors. The binding pocket is flexible and able to enlarge to accommodate the larger indole ring of 2 in addition to the larger halogen atom relative to 1. The combination of the ring system, halogen type and the flexible nature of the pocket may explain the higher affinity of 2 over 1 towards calpain-I. With increased hydrophobic contact with the protein, 2 will bind more tightly within the pocket. The two different conformations of 2 found in the structure of PEF(S) with the ligand bound indicate that specific bonding interactions with the NH group are not important for tight binding so that even larger aromatic ring systems could perhaps be accommodated.

Taken together, the flexibility of the binding site in accommo-dating different aromatic ring conformations and the lack of polar contacts with the surface of the protein suggest that significant scope exists to refine our inhibitor design. Since the mercaptoac-rylic acid unit does not seem to be directly involved in binding or establishing selectivity to PEF(S), it might be replaced with more synthetically accessible groups or used as a spacer to target other interactions of the protein surface. However, although both inhibitors bind to the calcium binding domain PEF(S) and are hence allosteric modulators of calpain-I, the second calcium binding domain within the heterodimeric structure, PEF(L), may also bind these compounds as it is very similar in structure and also con-tains a binding groove occupied by a helical domain of calpastatin in the inhibitory complex (Hanna et al., 2008). It is the binding of the inhibitors to this domain that may explain the discrepancy in inhibition constants between the two major calpain isoforms since PEF(S) is identical in calpains I and II (Adams et al., 2012) and the mercaptoacrylic acid may play a greater role in this inter-action. The inhibitors mode of action may disrupt the overall movement of the domains that occurs during the activation of the protease.

4. Conclusion

Since human calpain I is a potential drug target, it is preferable to study the interactions of inhibitors with the human form of the enzyme. Here we report the first crystal structure of human calpain PEF(S). For completeness we also redetermined the crystal struc-ture of unliganded-PEF(S) from Sus scrofa at 1.79 Å resolution (PDB: 4PHN) and found that it was highly similar to the structure of the human homologue. The excellent quality of the crystals obtained enabled solution of the structures to high resolution hence allowing observation of multiple conformations of the inhib-itors in the co-crystals.

The 2.03 and 2.05 Å structures of both (Z)-3-(5-bromoindol-3-yl)-2-mercaptoacrylic acid and (Z)-3-(4-chlorophenyl)-2-merca-ptoacrylic acid bound to the allosteric calcium binding domain PEF(S) revealed that the binding pocket is flexible enabling a mul-titude of van der Waals interactions to tightly bind the a-merca-ptoacrylic acids. To form hydrogen bonds the a-mercaptoacrylic acid moiety needs to remain in the plane of the aromatic ring but it seems likely that the hydrophilic interactions are not critical for the affinity of these compounds to the protein since they are only observed in one structure. Hydrophobic interactions are key for the stability of the complexes. With these new structures in hand new compounds can be developed that are more selective and potent inhibitors of both calpain-I and calpain II and used for the elucidation of the physiological role of the protease.

Acknowledgements

This work was supported by the UK's Engineering and Physical Sciences Research Council (EPSRC) and the Medical Research Coun-cil (MRC) through grant G0701192. We would like to thank Cardiff University and the EPSRC for the award of a Doctoral Prize Fellow-ship to SEA from DTG grant number EP/K502819/1. We are grateful to the EPSRC national mass spectrometry service at Swansea for mass spectroscopic analyses. The authors would like to thank Dia-mond Light Source for beamtime (proposal MX8096), and the staff of beamlines I03 and I04-1 for assistance with crystal testing and data collection.

References

Adams, S.E., Parr, C., Miller, D.J., Allemann, R.K., Hallett, M.B., 2012. Potent inhibition of Ca2+-dependent activation of calpain-1 by novel mercaptoacrylates. MedChemComm 3, 566–570.

Bailey, S., 1994. The Ccp4 suite – programs for protein crystallography. Acta Crystallogr., Sect. D 50, 760–763.

Blanchard, H., Grochulski, P., Li, Y., Arthur, J.S.C., Davies, P.L., Elce, J.S., Cygler, M., 1997. Structure of a calpain Ca2+-binding domain reveals a novel EF-hand and Ca2+-induced conformational changes. Nat. Struct. Biol. 4, 532–538.

Campbell, R.L., Davies, P.L., 2012. Structure–function relationships in calpains. Biochem. J. 447, 335–351.

Emori, Y., Kawasaki, H., Imajoh, S., Imahori, K., Suzuki, K., 1987. Endogenous inhibitor for calcium-dependent cysteine protease contains 4 internal repeats that could be responsible for its multiple reactive sites. Proc. Natl. Acad. Sci. U.S.A. 84, 3590–3594.

Emsley, P., Cowtan, K., 2004. Coot: model-building tools for molecular graphics. Acta Crystallogr., Sect. D 60, 2126–2132.

Evans, P., 2006. Scaling and assessment of data quality. Acta Crystallogr., Sect. D 62, 72–82.

Evans, P.R., Murshudov, G.N., 2013. How good are my data and what is the resolution? Acta Crystallogr., Sect. D 69, 1204–1214.

Goll, D.E., Thompson, V.F., Li, H., Wei, W., Cong, J., 2003. The calpain system. Physiol. Rev. 83, 731–801.

Hallett, M.B., Dewitt, S., 2007. Ironing out the wrinkles of neutrophil phagocytosis. Trends Cell Biol. 17, 209–214.

Hanna, R.A., Garcia-Diaz, B.E., Davies, P.L., 2007. Calpastatin simultaneously binds four calpains with different kinetic constants. FEBS Lett. 581, 2894–2898.

Hanna, R.A., Campbell, R.L., Davies, P.L., 2008. Calcium-bound structure of calpain and its mechanism of inhibition by calpastatin. Nature 456, 409–412.

Harwood, S.M., Yaqoob, M.M., Allen, D.A., 2005. Caspase and calpain function in cell death: bridging the gap between apoptosis and necrosis. Ann. Clin. Biochem. 42, 415–431.

Hosfield, C.M., Elce, J.S., Davies, P.L., Jia, Z.C., 1999. Crystal structure of calpain reveals the structural basis for Ca2+-dependent protease activity and a novel mode of enzyme activation. EMBO J. 18, 6880–6889.

Imajoh, S., Aoki, K., Ohno, S., Emori, Y., Kawasaki, H., Sugihara, H., Suzuki, K., 1988. Molecular-cloning of the Cdna for the large subunit of the high-Ca-2+-requiring form of human Ca-2+-activated neutral protease. Biochemistry-US 27, 8122–8128.

Lin, G.D., Chattopadhyay, D., Maki, M., Takano, E., Hatanaka, M., DeLucas, L., Narayana, S.V.L., 1997a. Purification, crystallization and preliminary X-ray diffraction studies of recombinant calcium-binding domain of the small subunit of porcine calpain. Acta Crystallogr., Sect. D 53, 474–476.

Lin, G.D., Chattopadhyay, D., Maki, M., Wang, K.K.W., Carson, M., Jin, L., Yuen, P., Takano, E., Hatanaka, M., DeLucas, L.J., Narayana, S.V.L., 1997b. Crystal structure of calcium bound domain VI of calpain at 1.9 angstrom resolution and its role in enzyme assembly, regulation, and inhibitor binding. Nat. Struct. Biol. 4, 539– 547.

Maki, M., Takano, E., Mori, H., Sato, A., Murachi, T., Hatanaka, M., 1987. All 4 internally repetitive domains of pig calpastatin possess inhibitory activities against calpain-I and calpain-Ii. FEBS Lett. 223, 174–180.

McCoy, A.J., 2007. Solving structures of protein complexes by molecular replacement with Phaser. Acta Crystallogr., Sect. D 63, 32–41.

Miller, D.J., Adams, S.E., Hallett, M.B., Allemann, R.K., 2013. Calpain-1 inhibitors for selective treatment of rheumatoid arthritis: what is the future? Future Med. Chem. 5, 2057–2074.

Murshudov, G.N., Vagin, A.A., Dodson, E.J., 1997. Refinement of macromolecular structures by the maximum-likelihood method. Acta Crystallogr., Sect. D 53, 240–255.

Ohno, S., Emori, Y., Suzuki, K., 1986. Nucleotide sequence of a cDNA coding for the small subunit of human calcium-dependent protease. Nucleic Acids Res. 14, 5559.

Orrenius, S., Zhivotovsky, B., Nicotera, P., 2003. Regulation of cell death: the calcium-apoptosis link. Nat. Rev. Mol. Cell Biol. 4, 552–565.

Potterton, E., Briggs, P., Turkenburg, M., Dodson, E., 2003. A graphical user interface to the CCP4 program suite. Acta Crystallogr., Sect. D 59, 1131–1137.

Saito, K.I., Elce, J.S., Hamos, J.E., Nixon, R.A., 1993. Widespread activation of calcium-activated neutral proteinase (calpain) in the brain in Alzheimer-disease – a potential molecular-basis for neuronal degeneration. Proc. Natl. Acad. Sci. U.S.A. 90, 2628–2632.

Sato, K., Kawashima, S., 2001. Calpain function in the modulation of signal transduction molecules. Biol. Chem. 382, 743–751.

Schollmeyer, J.E., 1988. Calpain II involvement in mitosis. Science 240, 911–913.

Schuttelkopf, A.W., van Aalten, D.M.F., 2004. PRODRG: a tool for high-throughput crystallography of protein-ligand complexes. Acta Crystallogr., Sect. D 60, 1355–1363.

Sorimachi, H., Hata, S., Ono, Y., 2011. Calpain chronicle-an enzyme family under multidisciplinary characterization. Proc. Jpn. Acad. B-Phys. 87, 287–327.

Storr, S.J., Carragher, N.O., Frame, M.C., Parr, T., Martin, S.G., 2011. The calpain system and cancer. Nat. Rev. Cancer 11, 364–374.

Strobl, S., Fernandez-Catalan, C., Braun, M., Huber, R., Masumoto, H., Nakagawa, K., Irie, A., Sorimachi, H., Bourenkow, G., Bartunik, H., Suzuki, K., Bode, W., 2000. The crystal structure of calcium-free human m-calpain suggests an electrostatic switch mechanism for activation by calcium. Proc. Natl. Acad. Sci. U.S.A. 97, 588–592.

Todd, B., Moore, D., Deivanayagam, C.C.S., Lin, G.D., Chattopadhyay, D., Maki, M., Wang, K.K.W., Narayana, S.V.L., 2003. A structural model for the inhibition of calpain by calpastatin: crystal structures of the native domain VI of calpain and its complexes with calpastatin peptide and a small molecule inhibitor. J. Mol. Biol. 328, 131–146.

Tontchev, A.B., Yamashima, T., 1999. Ischemic delayed neuronal death: role of the cysteine proteases calpain and cathepsins. Neuropathology 19, 356–365.

Wendt, A., Thompson, V.F., Goll, D.E., 2004. Interaction of calpastatin with calpain: a review. Biol. Chem. 385, 465–472.

Winter, G., 2010. Xia2: an expert system for macromolecular crystallography data reduction. J. Appl. Crystallogr. 43, 186–190.

Zhang, W.L., Lu, Q., Xie, Z.J., Mellgren, R.L., 1997. Inhibition of the growth of WI-38 fibroblasts by benzyloxycarbonyl-Leu-Leu-Tyr diazomethyl ketone: Evidence that cleavage of p53 by a calpain-like protease is necessary for G(1) to S-phase transition. Oncogene 14, 255–263.